GEOLOGY | THE GEOLOGICAL SOCIETY OF AMERICA®

https://doi.org/10.1130/G53151.1

Manuscript received 21 January 2025
Revised manuscript received 3 April 2025
Manuscript accepted 20 May 2025

Published online 3 June 2025

Coesite discovered in Australasian microtektites

L. Folco[1,2,*], E. Mugnaioli[1,2], M. Masotta[1,2], and B.P. Glass[3]
[1]Dipartimento di Scienze della Terra, Università di Pisa, 56126 Pisa, Italy
[2]Centro per la Integrazione della Strumentazione–Università di Pisa (CISUP), 56126 Pisa, Italy
[3]Department of Geosciences, University of Delaware, Newark, Delaware 19716, USA

ABSTRACT

Microtektites are microscopic glass spherules produced by large impacts on Earth. Whether they formed as impact melt droplets or as condensates from a target-dominated vapor plume is debated. Combining optical, scanning, and transmission electron microscopy, we studied microscopic silica-rich inclusions in four Australasian microtektites to search for high-pressure phases produced by shock metamorphism in the precursor materials. Three microtektites are from deep-sea sediment cores close to the putative impact location in Southeast Asia, and one is from the Transantarctic Mountains at the extreme reaches of the strewn field. Inclusions in the oceanic microtektites consist of a few partially resorbed microscopic quartz and coesite grains set in a silica-rich glass matrix; the latter hosts a multitude of individual nanoscopic coesite relicts. The inclusion in the Antarctic microtektite consists of featureless silica-rich glass, is devoid of coesite, and shows diffusive boundaries. Coesite grains in the deep-sea microtektites are interpreted as impact-melted relicts of larger crystals originally formed during shock metamorphism in a quartz-rich target precursor. The presence of coesite in deep-sea microtektites strengthens the argument that Australasian microtektites found closest to the impact location originated as impact melt spherules upon compression-decompression melting during impact cratering and not as target vapor plume condensates. The high degree of digestion of the inclusion in the Antarctic microtektite is in line with the view that the most distal Australasian microtektites experienced the highest thermal regimes.

INTRODUCTION

Tektites and microtektites are distal impact glass ejecta distributed in strewn fields extending as far as thousands of kilometers (e.g., Glass and Simonson, 2013). Numerical models predict that they form as an expanding spray of liquid droplets of mainly target materials that underwent melting, partial vaporization, high-velocity ejection, and fragmentation upon unloading from the high pressures generated by hypervelocity impacts of asteroidal or cometary bodies onto Earth's crust (e.g., Artemieva, 2002; Johnson and Melosh, 2012). Many aspects of this complex sequence of processes are still unclear when considering observations on natural samples. For instance, a widely accepted model, supported by the occurrence of partly digested inclusions of precursor materials (e.g., shocked quartz), vesicles, and compositional banding in Australasian microtektites, envisions that microtektites originated as impact melt droplets formed by compression-decompression melting during impact cratering (e.g., Folco et al., 2010; Glass et al., 2004). This model has been recently challenged. According to Koefoed et al. (2024), an origin as vapor condensate spherules best explains the K-isotopic systematics in Australasian microtektites. In addition, to account for the lack of impactor contamination in the most distal Australasian microtektites from Antarctica, Folco et al. (2024) suggested that they formed prior to impactor touchdown through the melting of the topmost layers of the target induced by radiative heating preceding the hypervelocity approach of a meteoritic projectile; in contrast, those ejected closer to the impact location (with as much as 5 wt% impactor contamination) formed upon touchdown by compression-decompression melting.

This work, based on optical, scanning, and transmission electron microscopy analyses, provides the first report of coesite—a high-pressure polymorph of silica—in Australasian microtektites. Coesite was found in quartz and lechatelierite (silica glass) microscopic inclusions. This finding has implications on the formation model of impact coesite in distal ejecta and on the debated impact melting versus condensation origin of microtektites.

THE AUSTRALASIAN STREWN FIELD

The Australasian tektite and microtektite strewn field covers ~15% of Earth's surface (Fig. 1) and formed ca. 0.8 Ma (Jourdan et al., 2019) through the hypervelocity impact of a chondritic body (e.g., Goderis et al., 2017; Folco et al., 2023). It is the youngest and the largest of the five Cenozoic strewn fields known: Australasian, Ivory Coast, Central European, Central America, and North America (Glass and Simonson, 2013; Rochette et al., 2021). Nonetheless, its source crater has not yet been identified. Evidence of high-pressure phases in tektites (Cavosie et al., 2018; Glass et al., 2020; Masotta et al., 2020) and other shocked ejecta (e.g., Glass and Fries, 2008) indicates that tektites and microtektites are linked to a crater-forming event. Petrographic and geochemical trends (geographic distribution of microtektite abundance and of Muong Nong–type tektites and their ^{10}Be concentrations) point to an impact location in Indochina or the surrounding seas (Ma et al., 2004; Glass and Koeberl, 2006; Prasad et al., 2007) or farther north in northwest China (Mizera, 2022). Ejecta distribution suggests a crater diameter ≥30 km (Glass and Koeberl, 2006; Prasad et al., 2007).

SAMPLES AND METHODS

Several studies of systematic variations of petrographic and geochemical features with ejection distance (e.g., Goderis et al., 2017; Rochette et al., 2018; Chernonozhkin et al., 2021; Folco

L. Folco https://orcid.org/0000-0002-7276-3483
E. Mugnaioli https://orcid.org/0000-0001-9543-9064
M. Masotta https://orcid.org/0000-0003-2463-8116
B.P. Glass https://orcid.org/0000-0002-7126-8974
*luigi.folco@unipi.it

CITATION: Folco, L., et al., 2025, Coesite discovered in Australasian microtektites: Geology, v. XX, p. , https://doi.org/10.1130/G53151.1

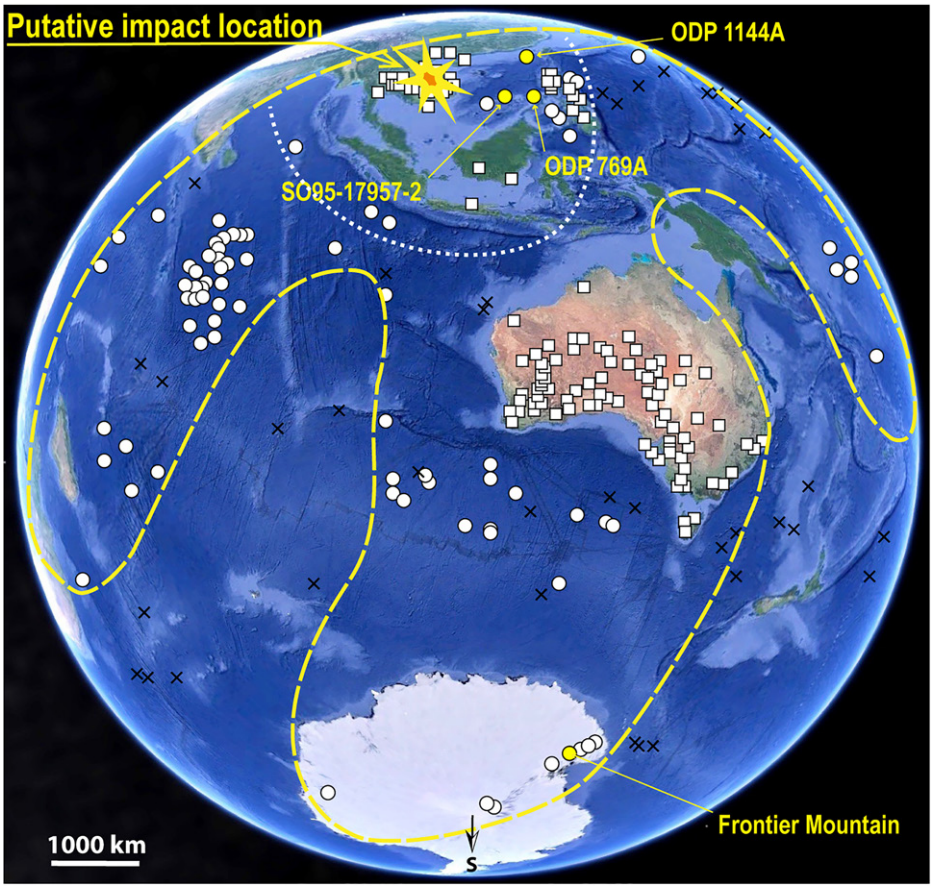

Figure 1. Australasian tektites and microtektites strewn field (outlined by yellow dashed line; after Folco et al., 2023). Find locations of tektites and microtektites are marked by squares and circles, respectively; yellow circles are locations of microtektites studied in this work. Arrow indicates putative impact location in Indochina (Ma et al., 2004). Black crosses are locations of deep-sea sediment cores where microtektites were not found. White dotted line envelopes the region where petrographic evidence for high pressure has been found so far (see text for details).

et al., 2024) have contributed to a better understanding of the complex interplay of impact melting, high-velocity ejection and fragmentation, vaporization, condensation, and re-entry heating in the formation of tektites and microtektites. For this reason, the studied samples include three Australasian microtektites from deep-sea sediments (AUS-DSS) close to the putative impact location in Southeast Asia (core SO95-17957-2, Ocean Drilling Program [ODP] Hole 769A, and ODP Hole 1144A) and one from Frontier Mountain (FRO) in the Transantarctic Mountains (AUS-ANT) at the extreme reaches of the strewn field as currently mapped (Table 1). Our petrographic investigation was conducted combining optical microscopy, microanalytical scanning electron microscopy (SEM), dual beam microscopy (DB), and microanalytical transmission electron microscopy (TEM) coupled with three-dimensional electron diffraction (3DED; Mugnaioli and Gemmi, 2018) at Centro per la Integrazione della Strumentazione–Università di Pisa (CISUP). Major and trace element concentrations, used here for microtektite classification purposes, were determined in microtektites ODP 769A,15_26 and FRO 2.9-1 by laser-ablation–inductively coupled plasma–mass spectrometry (LA-ICP-MS) at CISUP; those for the other two microtektites are from the literature (Table S1 in the Supplemental Material[1]). Further details on samples and methods are given in the Supplemental Material.

RESULTS

The AUS-DSS microtektites studied here have spheroid shapes, dark-brown color, translucent luster, abundant inclusions as large as a few tens of micrometers dominated by silica phases, compositional bands (schlieren), and vesicles (Table 1). They range in size from 350 to 700 μm in maximum elongation (Fig. 2; Figs. S1–S2). Microtektites SO95-17957-2,04 and ODP 1144A,01 have normal composition, whereas ODP 769A,15_26 is of the high-Ni variety (Ni = 232 μg/g). The AUS-ANT microtektite is a pale-yellow transparent sphere 485 μm in diameter with normal composition (Table 1), devoid of vesicles, with only one microscopic (few tens of micrometers across) silica-rich inclusion with diffuse boundaries. Overall, the AUS-ANT microtektite is representative of the petrographic characteristics of the Australasian microtektites from Antarctica described in the literature ($n = 219$; e.g., Folco et al. 2010, 2023), but it is the only known one

[1]Supplemental Material. Analytical methods, Table S1 with geochemical data, and Figures S1–S4. Please visit https://doi.org/10.1130/GEOL.S.29132141 to access the supplemental material; contact editing@geosociety.org with any questions.

TABLE 1. RECOVERY LOCATION, MAIN PETROGRAPHIC FEATURES, AND GEOCHEMICAL CLASSIFICATION OF THE AUSTRALASIAN MICROTEKTITES STUDIED IN THIS WORK

Name	SO95-17957-2,04	ODP 769A,15_26	ODP 1144A,01	FRO 2.9-1
Recovery location				
Site	Core SO95-17957-2	ODP Hole 769A	ODP Hole 1144A	Frontier Mountain
Region	South China Sea	Sulu Sea	South China Sea	Transantarctic Mountains
Latitude	10.90°N	8.79°N	20.05°N	72.98°S
Longitude	115.31°E	121.22°E	117.42°E	160.33°E
Distance (km) from putative impact location at 17°N, 107°E*	1181	1789	1149	10,700
Petrographic features and chemical type				
Shape	Teardrop	Prolate ellipsoid	Broken teardrop	Sphere
Size (μm)	450 × 215	360 × 280	707 × 629	485
Color	Pale brown	Dark brown	Brown	Pale yellow
Transparency	Translucent	Translucent	Translucent	Transparent
Microscopic inclusions	Lechatelierite, quartz, coesite	Lechatelierite, quartz, coesite	Lechatelierite, quartz, coesite	Si-rich glass
Microscopic vesicles	Several	Many	Few	None
Microscopic schlieren	Abundant	Some	Abundant	None
Compositional type†	Normal	High-Ni	Normal	Normal

Note: ODP—Ocean Drilling Program.
*Putative impact location from Ma et al. (2004).
†Classification scheme according to Glass et al. (2004). Normal type: MgO <6 wt%. High-Ni type: normal type composition but with Ni >100 μg/g.

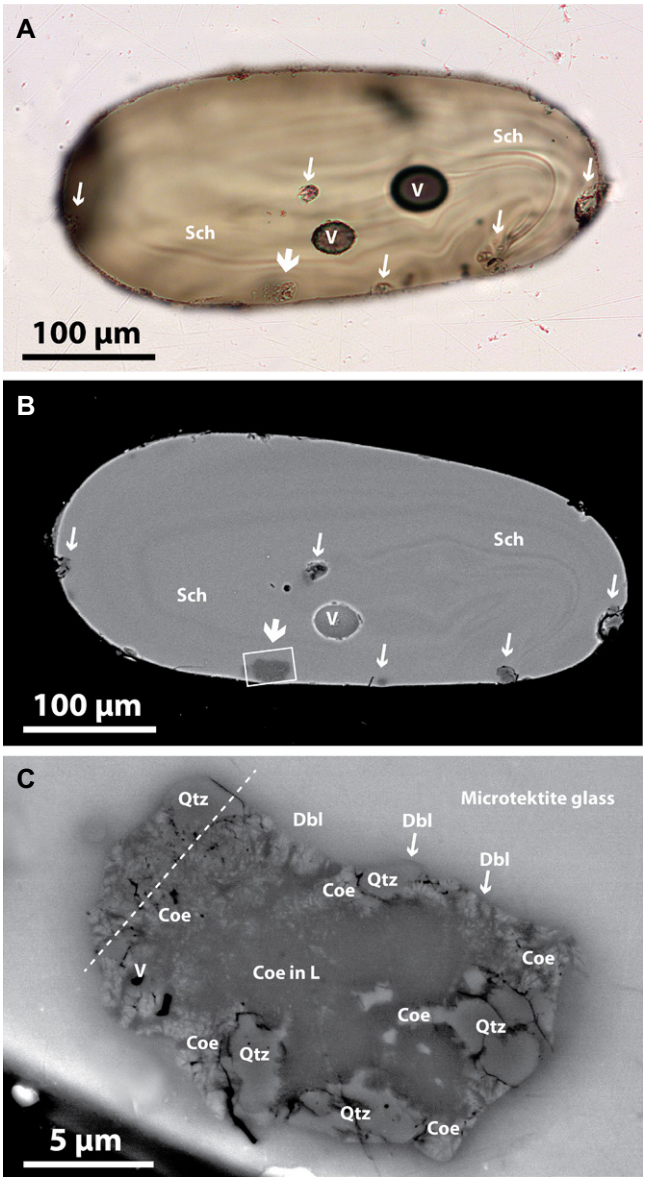

Figure 2. Micrographs of sectioned Australasian microtektite SO95-17957-2,04. (A) Microtektite is pale brown with teardrop shape. It shows folded schlieren (Sch), microscopic vesicles (V), and mineral inclusions (arrowed). Thick white arrow points to inclusion studied in this work. Optical microscope image, plane polarized light. (B) Same petrographic features as in A in backscattered electron (BSE) image. White rectangle outlines field of view of image in panel C. (C) Close-up BSE image of a quartz (Qtz) + lechatelierite (L) + coesite (Coe) inclusion. Silica phases in the inclusion can be distinguished by their different electron density contrast, which increases from lechatelierite to quartz to coesite. A diffusive boundary layer (Dbl) discontinuously surrounds the inclusion. Dashed line traces location of the dual beam microscopy section studied in this work.

with a documented silica-rich inclusion (Folco et al., 2009).

As viewed under SEM (Fig. 2), the inclusions in the AUS-DSS microtektites consist of microscopic quartz grains and submicroscopic coesite grains set in vesiculated lechatelierite (Table S1) in variable proportions. Diffusive boundary layers a few micrometers in thickness surround the inclusions. As exemplified by microtektite SO95-17957-2,04, quartz grains are typically found at the edge of the inclusions and are surrounded by coesite, whereas lechatelierite typically dominates the cores of the inclusions. The quartz grains are anhedral and commonly fractured. The surrounding coesite forms polycrystalline aggregates of nanoscopic crystals set in silica glass. Moving toward the lechatelierite at the core of the inclusion, the coesite grain size becomes smaller and the interstitial silica glass–to–coesite volume ratio increases, resulting in irregular, finely fringed contacts. The central part of the inclusion is dominated by lechatelierite that contains abundant, scattered nanoscopic grains of coesite. The inclusions in the other two AUS-DSS microtektites ODP 769A,15_26 and ODP 1144A,01 are more vesiculated yet characterized by similar microstructural zoning (Figs. S1 and S2).

The DB cross section of microtektite SO95-17957-2,04 samples the microstructural zoning described above (Fig. 3). Under TEM, coesite is identified through 3DED and characteristically shows (010) polysynthetic twinning. Coesite forms euhedral crystals overgrowing the quartz grains at the edge of the inclusion (Fig. 3B). Moving toward the lechatelierite core, coesite is segmented in submicroscopic tabular grains by a fine network of silica glass veinlets producing the polycrystalline aggregates seen under SEM (Fig. 3C). They closely resemble the tartan-like textures observed in symplectic regions (microcrystalline coesite aggregates in silica glass) in shocked porous sandstones (e.g., Folco et al., 2018; Kieffer et al., 1976). The amount of interstitial silica glass increases toward the lechatelierite inclusion core, while disaggregation of larger coesite grains produces anhedral nanoscopic grains seemingly floating freely in the lechatelierite core. The TEM images of the DB section from microtektites ODP 1144A1,01 and ODP 769A,15_26 show that the nanoscopic coesite grains scattered through the lechatelierite are elongated parallel to the (010) twinning, anhedral with embayed grain boundaries, and in some cases broken apart (Figs. 3E and 3F).

As viewed under SEM, the silica-rich inclusion in the AUS-ANT microtektite FRO 2.9-1 consists of featureless glass (Fig. S3). The contact with the host microtektite glass is diffuse. Its bulk composition is dominated by SiO_2 (92.5 wt%) with lesser amounts of Al_2O_3 (3.8 wt%) and FeO (1.29 wt%) and minor MgO, TiO_2, CaO, K_2O, and Na_2O. TEM observations confirm the homogeneous nature of the silica-rich glass seen at the SEM scale (Fig. S3).

DISCUSSION

Coesite is a common product of shock metamorphism associated with impact cratering on quartz-bearing target rocks. The preservation of coesite as a metastable phase in shocked rocks that experienced peak pressures and temperatures much beyond its stability field (i.e., pressures of 3–10 GPa and temperatures <2700 °C) has been a controversial issue since its discovery by Chao et al. (1960). Current models for its formation are (1) crystallization from a silica impact melt during shock unloading, when the pressure release path passes through the coesite stability field (e.g., Langenhorst, 2003; Chen et al., 2010); (2) subsolidus nucleation from highly densified diaplectic silica glass (Stähle et al., 2008); and (3) direct quartz-coesite subsolidus transformation during the prograde path of shock metamorphism (Kiefer et al., 1976; Folco et al., 2018; Campanale et al., 2021). Models 1 and 2 are based on the study of nonporous target rocks and single quartz crystals, while model 3 is based on the study of porous sandstones.

In our interpretation, the euhedral grains of coesite overgrowing quartz cores (Fig. 3B) indicate formation through direct quartz-coesite subsolidus transformation. The adjacent polycrystalline aggregates consisting of submicroscopic elongated grains of coesite pervaded by silica glass veinlets indicate local incipient melting of coesite (Fig. 3B). The nanoscopic anhedral (in some cases broken apart) coesite grains dispersed in the surrounding lechatelierite are interpreted as relicts of more pronounced melting and disaggregation of the polycrystalline coesite aggregates (Figs. 3B, 3D, and 3F). Nanocrystalline coesite is thus a relict of the melting of

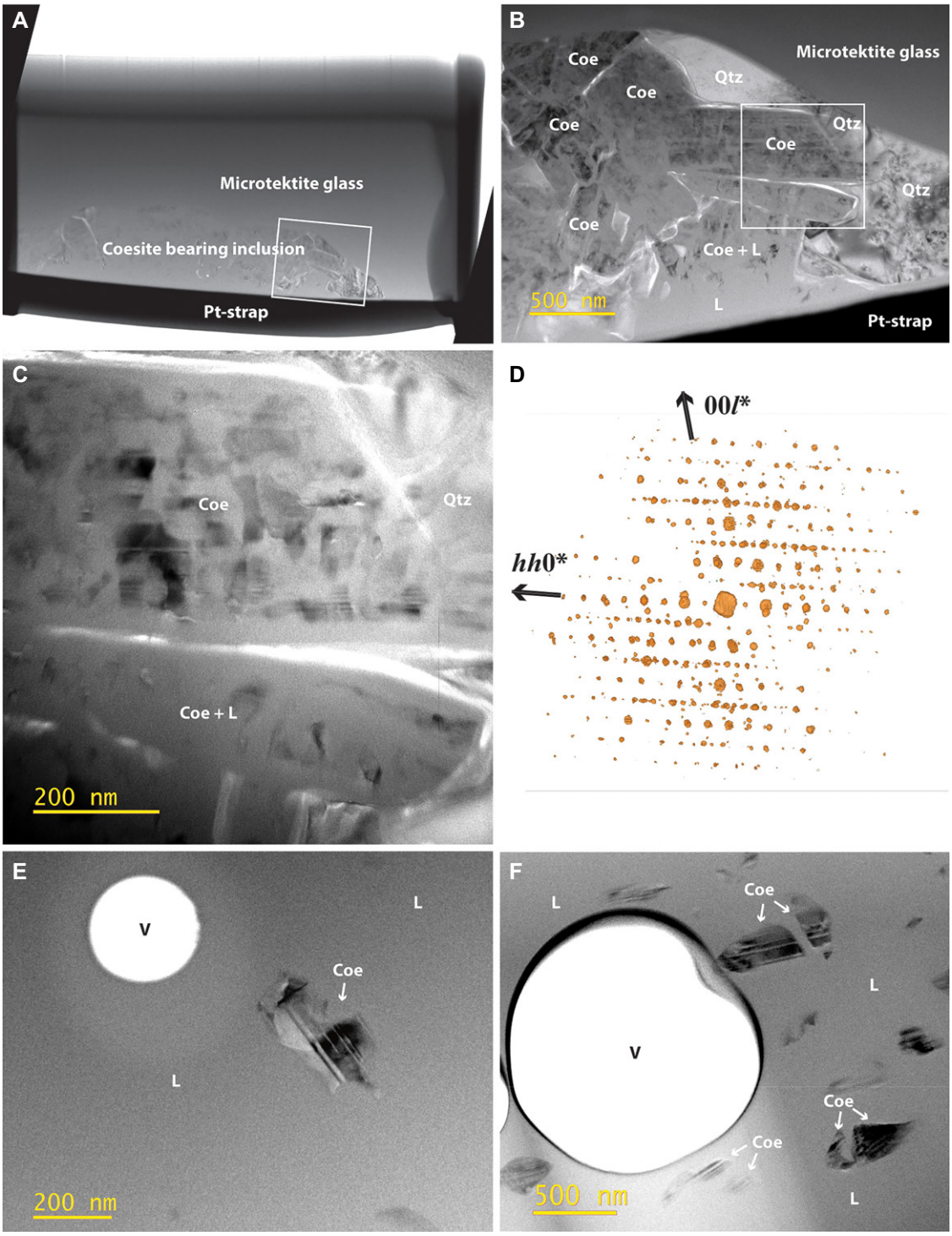

Figure 3. Transmission electron microscopy images of electron transparent dual beam microscopy section of quartz + lechatelierite + coesite inclusions from Australasian deep-sea sediment microtektites. (A) Whole section of coesite-bearing inclusion in microtektite SO95-17957-2,04. White rectangle outlines area featured in panel B. (B) Textural relationships between quartz (Qtz), coesite (Coe), and lechatelierite (L). Few microscopic quartz relicts at periphery of inclusion are overgrown by euhedral coesite grains with polysynthetic (010) twinning. Toward the core of the inclusion dominated by lechatelierite, coesite is segmented by a network of silica glass veinlets producing polycrystalline aggregates, which then disaggregate with increasing amount of silica glass. White rectangle traces area featured panel C. (C) Close-up view of euhedral coesite (top) adjacent to polycrystalline aggregate with subhedral outline (bottom). (D) Reconstruction of reciprocal space sampled by three-dimensional electron diffraction from a twinned coesite grain. This picture displays a view of the diffraction volume along $\bar{h}h0$ vector. Projections of $00l^*$ and $hh0^*$ vectors are indicated. (E) Nanoscopic anhedral coesite grain with embayed crystal boundaries embedded in lechatelierite in microtektite ODP 769A,15_26. (F) Several nanoscopic anhedral coesite grains dispersed in an area of ~2 μm² of lechatelierite in microtektite ODP 1144A,01. Broken-apart grains are arrowed. V—vesicle.

pre-existing larger coesite grains formed in subsolidus conditions during shock metamorphism (model 3). Coesite disaggregation in elongated subgrains could result from preferential melting of planar deformation features present in the quartz precursor (Folco et al., 2018).

The preservation of coesite constrains the cooling history of the Australasian microtektites found close to the putative impact location in Southeast Asia. Experiments (Walter, 1965) suggest that a maximum quench time of 10 s is required to prevent the full transformation of coesite into cristobalite at high temperature. Due to the lack of cristobalite in the studied inclusions, we infer a much more rapid quench, possibly assisted by endothermic reactions of melting (quartz and coesite melt to form lechatelierite) and vesicle expansion (Masotta et al., 2020).

There is general consensus that the abundant quartz and lechatelierite inclusions found in Australasian tektites and microtektites are relicts of the fusion of a quartz-bearing target material upon impact melting (e.g., Glass and Simonson, 2013). Diffusive boundary layers observed at the contact between the inclusion and the host microtektite glass (Fig. 2C; Fig. S3) indicate variable degrees of digestion. The nonvolatile component of the microtektite glass bulk composition and of the silica glass in the inclusions lies on a mixing line (Fig. S1). The finding of coesite in AUS-DSS microtektites strengthens the argument that Australasian microtektites found closest to the impact location originated as impact melt spherules upon compression/decompression melting during impact cratering (Glass and Simonson, 2013; Folco et al.,

2010) and not as condensates from a vaporized target as recently proposed in the literature (Koefoed et al., 2024). The lack of coesite in the AUS-ANT microtektite could be due to complete resorption induced by severe heating during impact melting and possibly deceleration in ambient air or atmospheric re-entry, suggested to explain the paucity of mineral inclusions, vesicles, and schlieren, and moderately volatile element and Fe-isotope distribution in the most distal microtektites (Folco et al., 2010; Chernonozhkin et al., 2021; Del Rio et al., 2025). The lack of evidence for high pressure in the AUS-ANT microtektite is also consistent with the view (Folco et al., 2024) that the most distally ejected Australasian microtektites formed earliest as high-temperature impact melt droplets through radiative heating prior to impactor touchdown.

The finding of high-pressure evidence in microtektites from the South China Sea and Solu Sea (i.e., coesite; this work) in microscopic ejecta in the South China Sea (i.e., coesite, planar deformation features in quartz, TiO_2-II; Glass and Fries, 2008; Campanale et al., 2019, 2024) and in tektites from Thailand (i.e., granular zircon; Cavosie et al., 2018) and Laos (Walter, 1965; Glass et al., 2020; Masotta et al., 2020; Fig. 1) strengthens the view that the source crater is likely located in Southeast Asia.

ACKNOWLEDGMENTS

Australasian microtektite research at the University of Pisa is supported by the Italian National Programme for Antarctic Research (PNRA), project Meteoriti Antartiche, ID# PNRA16_00029, and by the Italian Space Agency—Ministry of University and Research (ASI–MUR) projet SpaceItUp!, Project Contract n. 212 2024-5-E.0 - CUP n. I53D24000060005. The paper benefited from the constructive reviews by Aaron Cavosie, Kieren Howard, and Uwe Reimold. Science editor Tracy Rushmer is thanked for handling the manuscript.

REFERENCES CITED

Artemieva, N., 2002, Tektite origin in oblique impacts: Numerical modeling of the initial stage, *in* Plado, J., and Pesonen, L.J., eds., Impacts in Precambrian Shields: Berlin, Springer, p. 257–276, https://doi.org/10.1007/978-3-662-05010-1_10.

Campanale, F., Mugnaioli, E., Folco, L., Gemmi, M., Lee, M.R., Daly, L., and Glass, B.P., 2019, Evidence for subsolidus quartz-coesite transformation in impact ejecta from the Australasian tektite strewn field: Geochimica et Cosmochimica Acta, v. 264, p. 105–117, https://doi.org/10.1016/j.gca.2019.08.014.

Campanale, F., Mugnaioli, E., Gemmi, M., and Folco, L., 2021, The formation of impact coesite: Scientific Reports, v. 11, 16011, https://doi.org/10.1038/s41598-021-95432-6.

Campanale, F., Mugnaioli, E., Folco, L., Parlanti, P., and Gemmi, M., 2024, TiO_2 II: The high-pressure Zr-free srilankite endmember in impact rocks: Meteoritics & Planetary Science, v. 59, p. 529–543, https://doi.org/10.1111/maps.14137.

Cavosie, A.J., Timms, N.E., Erickson, T.M., and Koeberl, C., 2018, New clues from Earth's most elusive impact crater: Evidence of reidite in Australasian tektites from Thailand: Geology, v. 46, p. 203–206, https://doi.org/10.1130/G39711.1.

Chao, E.C.T., Shoemaker, E.M., and Madsen, B.M., 1960, First natural occurrence of coesite: Science, v. 132, p. 220–222, https://doi.org/10.1126/science.132.3421.220.

Chen, M., Xiao, W., and Xie, X., 2010, Coesite and quartz characteristic of crystallization from shock-produced silica melt in the Xiuyan crater: Earth and Planetary Science Letters, v. 297, p. 306–314, https://doi.org/10.1016/j.epsl.2010.06.032.

Chernonozhkin, S.M., et al., 2021, Isotopic evolution of planetary crusts by hypervelocity impacts evidenced by Fe in microtektites: Nature Communications, v. 12, 5646, https://doi.org/10.1038/s41467-021-25819-6.

Del Rio, M., Folco, L., Mugnaioli, E., Goderis, S., and Masotta, M., 2025, Loss and accretion of moderately volatile elements K and Na in Australasian microtektites from Antarctica: Geochimica et Cosmochimica Acta, v. 395, p. 212–228, https://doi.org/10.1016/j.gca.2025.03.005.

Folco, L., D'Orazio, M., Tiepolo, M., Tonarini, S., Ottolini, L., Perchiazzi, N., Rochette, P., and Glass, B.P., 2009, Transantarctic Mountain microtektites: Geochemical affinity with Australasian microtektites: Geochimica et Cosmochimica Acta, v. 73, p. 3694–3722, https://doi.org/10.1016/j.gca.2009.03.021.

Folco, L., Perchiazzi, N., D'Orazio, M., Frezzotti, M.L., Glass, B.P., and Rochette, P., 2010, Shocked quartz and other mineral inclusions in Australasian microtektites: Geology, v. 38, p. 211–214, https://doi.org/10.1130/G30512.1.

Folco, L., Mugnaioli, E., Gemelli, M., Masotta, M., and Campanale, F., 2018, Direct quartz-coesite transformation in shocked sandstone from Kamil Crater (Egypt): Geology, v. 46, p. 739–742, https://doi.org/10.1130/G45116.1.

Folco, L., Rochette, P., D'Orazio, M., and Masotta, M., 2023, The chondritic impactor origin of the Ni-rich component in Australasian tektites and microtektites: Geochimica et Cosmochimica Acta, v. 360, p. 231–240, https://doi.org/10.1016/j.gca.2023.09.018.

Folco, L., Masotta, M., Rochette, P., Del Rio, M., and Di Vincenzo, G., 2024, Australasian microtektites: Early target-projectile interaction in large impacts on Earth: Geochemical Perspectives Letters, v. 31, p. 22–26, https://doi.org/10.7185/geochemlet.2427.

Glass, B.P., and Fries, M., 2008, Micro-Raman spectroscopic study of fine-grained, shock-metamorphosed rock fragments from the Australasian microtektite layer: Meteoritics & Planetary Science, v. 43, p. 1487–1496, https://doi.org/10.1111/j.1945-5100.2008.tb01023.x.

Glass, B.P., and Koeberl, C., 2006, Australasian microtektites and associated impact ejecta in the South China Sea and the Middle Pleistocene supereruption of Toba: Meteoritics & Planetary Science, v. 41, p. 305–326, https://doi.org/10.1111/j.1945-5100.2006.tb00211.x.

Glass, B.P., and Simonson, B.M., 2013, Distal Impact Ejecta Layers: A Record of Large Impacts in Sedimentary Deposits: Berlin, Heidelberg, Springer, 716 p., https://doi.org/10.1007/978-3-540-88262-6

Glass, B.P., Huber, H., and Koeberl, C., 2004, Geochemistry of Cenozoic microtektites and clinopyroxene-bearing spherules: Geochimica et Cosmochimica Acta, v. 68, p. 3971–4006, https://doi.org/10.1016/j.gca.2004.02.026.

Glass, B.P., Folco, L., Masotta, M., and Campanale, F., 2020, Coesite in a Muong Nong-type tektite from Muong Phin, Laos: Description, formation, and survival: Meteoritics & Planetary Science, v. 55, p. 253–273, https://doi.org/10.1111/maps.13433.

Goderis, S., Tagle, R., Fritz, J., Bartoschewitz, R., and Artemieva, N., 2017, On the nature of the Ni-rich component in splash-form Australasian tektites: Geochimica et Cosmochimica Acta, v. 217, p. 28–50, https://doi.org/10.1016/j.gca.2017.08.013.

Johnson, B.C., and Melosh, H.J., 2012, Formation of spherules in impact produced vapor plumes: Icarus, v. 217, p. 416–430, https://doi.org/10.1016/j.icarus.2011.11.020.

Jourdan, F., Nomade, S., Wingate, M.T.D., Eroglu, E., and Deino, A., 2019, Ultraprecise age and formation temperature of the Australasian tektites constrained by $^{40}Ar/^{39}Ar$ analyses: Meteoritics & Planetary Science, v. 54, p. 2573–2591, https://doi.org/10.1111/maps.13305.

Kieffer, S.W., Phakey, P.P., and Christie, J.M., 1976, Shock processes in porous quartzite: Transmission electron microscopy and theory: Contributions to Mineralogy and Petrology, v. 59, p. 41–93, https://doi.org/10.1007/BF00375110.

Koefoed, P., Folco, L., Di Vincenzo, G., Nie, N.X., Glass, B.P., Neuman, M., and Wang, K., 2024, Understanding microtektite formation: Potassium isotope evidence for condensation in a vapor plume: Geochimica et Cosmochimica Acta, v. 379, p. 23–38, https://doi.org/10.1016/j.gca.2024.06.015.

Langenhorst, F., 2003, Nanostructures in ultrahigh-pressure metamorphic coesite and diamond: A genetic fingerprint: Mitteilungen der Österreichische Mineralogische Gesellschaft, v. 148, p. 401–412.

Ma, P., et al., 2004, Beryllium-10 in Australasian tektites: Constraints on the location of the source crater: Geochimica et Cosmochimica Acta, v. 68, p. 3883–3896, https://doi.org/10.1016/j.gca.2004.03.026.

Masotta, M., et al., 2020, 3D X-ray tomographic analysis reveals how coesite is preserved in Muong Nong-type tektites: Scientific Reports, v. 10, 20608, https://doi.org/10.1038/s41598-020-76727-6.

Mizera, J., 2022, Quest for the Australasian impact crater: Failings of the candidate location at the Bolaven Plateau, Southern Laos: Meteoritics & Planetary Science, v. 57, p. 1973–1986, https://doi.org/10.1111/maps.13912.

Mugnaioli, E., and Gemmi, M., 2018, Single-crystal analysis of nanodomains by electron diffraction tomography: Mineralogy at the order-disorder borderline: Zeitschrift für Kristallographie, v. 233, p. 163–178, https://doi.org/10.1515/zkri-2017-2130.

Prasad, M.S., Mahale, V.P., and Kodagali, V.N., 2007, New sites of Australasian microtektites in the central Indian Ocean: Implications for the location and size of source crater: Journal of Geophysical Research, v. 112, E06007, https://doi.org/10.1029/2006JE002857.

Rochette, P., Braucher, R., Folco, L., Horng, C.S., Aumaître, G., Bourlès, D.L., and Keddadouche, K., 2018, ^{10}Be in Australasian microtektites compared to tektites: Size and geographic controls: Geology, v. 46, p. 803–806, https://doi.org/10.1130/G45038.1.

Stähle, V., Altherr, R., Koch, M., and Nasdala, L., 2008, Shock-induced growth and metastability of stishovite and coesite in lithic clasts from suevite of the Ries impact crater (Germany): Contributions to Mineralogy and Petrology, v. 155, p. 457–472, https://doi.org/10.1007/s00410-007-0252-2.

Walter, L.S., 1965, Coesite discovered in tektites: Science, v. 147, p. 1029–1032, https://doi.org/10.1126/science.147.3661.1029.

Printed in the USA